Role of the MoFe Protein α-Subunit Histidine-195 Residue in FeMo-Cofactor Binding and Nitrogenase Catalysis†

Chul-Hwan Kim, William E. Newton, and Dennis R. Dean*

Department of Biochemistry and Anaerobic Microbiology, Virginia Polytechnic Institute and State University, Blacksburg, Virginia 24061

Received June 24, 1994; Revised Manuscript Received September 14, 1994®

ABSTRACT: Site-directed mutagenesis and gene-replacement procedures were used to isolate mutant strains of *Azotobacter vinelandii* that produce altered MoFe proteins in which the α-subunit residue-195 position, normally occupied by a histidine residue, was individually substituted by a variety of other amino acids. Structural studies have revealed that this histidine residue is associated with the FeMo-cofactor binding domain and probably provides an NH→S hydrogen bond to a central bridging sulfide located within FeMo-cofactor. Substitution by a glutamine residue results in an altered MoFe protein that binds but does not reduce N_2, the physiological substrate. Although N_2 is not a substrate for the altered MoFe protein, it is a potent inhibitor of both acetylene and proton reduction, both of which are otherwise effectively reduced by the altered MoFe protein. This result provides evidence that N_2 inhibits proton and acetylene reduction by simple occupancy of a common active site. N_2 also uncouples MgATP from proton reduction catalyzed by the altered MoFe protein but does so without lowering the overall rate of MgATP hydrolysis. Thus, the quasi-unidirectional flow of electrons from the Fe protein to the MoFe protein that occurs during nitrogenase turnover is controlled, in part, by the substrate serving as an effective electron sink. Substitution of the α-histidine-195 residue by glutamine also imparts to the altered MoFe protein hypersensitivity of both its acetylene reduction and N_2 binding to inhibition by CO, indicating that the imidazole group of the α-histidine-195 residue might protect an Fe contained within the FeMo-cofactor from attack by CO. Finally, comparisons of the catalytic and spectroscopic properties of altered MoFe proteins produced by various mutant strains suggest that the α-histidine-195 residue has a structural role, which serves to keep FeMo-cofactor attached to the MoFe protein and to correctly position FeMo-cofactor within the polypeptide matrix, such that N_2 binding is accommodated.

Biological nitrogen fixation is catalyzed by nitrogenase, an enzyme composed of two metal-containing component proteins called the Fe protein and the MoFe protein. During catalysis, electrons are delivered one at a time from the Fe protein to the MoFe protein in a process involving component−protein association and dissociation and hydrolysis of at least two MgATP for each electron transfer. Among the important questions attached to nitrogen fixation research are understanding (i) the structures of the metal centers that participate in electron transfer and/or substrate binding, (ii) the organization of the metalloclusters within the polypeptides and the contribution of those corresponding polypeptide environments to substrate binding and electron transfer, and (iii) the integration of MgATP binding and hydrolysis with intermolecular electron transfer. Considerable insight concerning these issues has been gained by recent reports on the three-dimensional structures of both nitrogenase component proteins (Georgiadis *et al.*, 1992; Kim & Rees 1992a,b; Kim *et al.*, 1993; Bolin *et al.*, 1993), and this insight has been summarized in recent review articles (Kim & Rees, 1994; Dean *et al.*, 1993).

There is compelling evidence that one of the metalloclusters contained within the MoFe protein, called FeMo-cofactor (Shah & Brill, 1977), provides the substrate-binding and -reduction sites (Shah & Brill, 1977; Rawlings *et al.*, 1978; Hawkes *et al.*, 1984; Scott *et al.*, 1990). FeMo-cofactor is currently modeled as having a metal−sulfide core constructed from sulfide-bridged $MoFe_3S_3$ and Fe_4S_3 subcluster fragments (Kim & Rees, 1992a; Chan *et al.*, 1993; also see Figure 1). In addition to its metal−sulfide core, FeMo-cofactor also contains an organic constituent, homocitrate (Hoover *et al.*, 1989), which is covalently attached to the Mo atom through its 2-hydroxyl and 2-carboxyl groups. Prior to the availability of direct structural information, we proposed a model (Dean & Jacobson, 1992; Dean *et al.*, 1990a,b; Scott *et al.*, 1992) based primarily on deduced amino-acid sequence comparisons and amino-acid substitution studies, where certain of the amino-acid residues contained within the MoFe protein α-subunit from *Azotobacter vinelandii* were targeted as being located within the FeMo-cofactor-binding domain. These residues were suggested to have structural roles in positioning FeMo-cofactor within the polypeptide pocket and to have potential catalytic functions in fine tuning FeMo-cofactor's electronic features. Relevant to the present work, an altered MoFe protein, which has an asparagine substitution for the interspecifically conserved α-histidine-195 residue, was shown to exhibit significantly changed catalytic and spectroscopic properties (Scott *et al.*, 1990, 1992). The subsequent structural models confirmed that this α-histidine

† The majority of this work was supported by a grant from the National Institutes of Health (DK37255). C.-H.K. was supported in part by a grant from the National Science Foundation (MCB9303800).

* To whom correspondence should be addressed. Tel.: (703) 231 5895. Fax: (703) 231 7126.

® Abstract published in *Advance ACS Abstracts,* February 1, 1995.

0006-2960/95/0434-2798$09.00/0

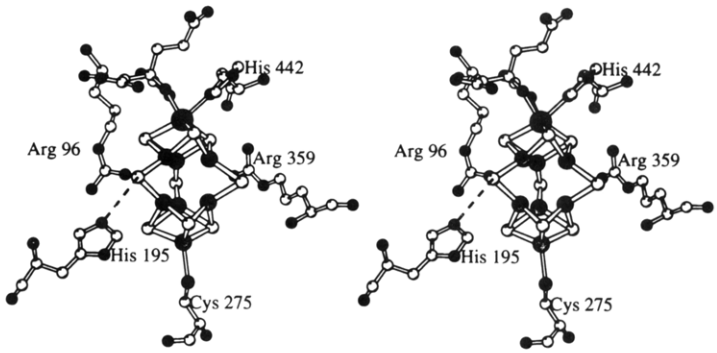

FIGURE 1: Stereoscopic view of FeMo-cofactor and selected polar residues in its environment. FeMo-cofactor is ligated to two protein residues, α-442^{His} and α-275^{Cys}. Also interacting closely with FeMo-cofactor are α-96^{Arg}, α-195^{His}, and α-359^{Arg}. A molecule of homocitrate provides two bonds to the Mo atom of FeMo-cofactor and is shown in the upper portion of the figure. An NH→S hydrogen bond of α-195^{His} to FeMo-cofactor is represented by a dashed line. The largest and darkest of the spheres in FeMo-cofactor is the Mo atom. The spheres of intermediate size and shade are Fe atoms, while the smallest and lightest spheres represent S atoms. In the homocitrate and protein components, C atoms are unshaded, whereas the O and N atoms are the same, darker shade. The figure was generated with the program MOLSCRIPT (Kraulis, 1991).

residue is closely associated with FeMo-cofactor, but it is apparently not bonded covalently to the FeMo-cofactor. In the present study, several new mutant strains, which produce altered MoFe proteins that have other amino acids substituted for the α-histidine-195 residue, were constructed. The effect of these amino-acid substitutions on the catalytic and spectroscopic features of the altered MoFe proteins produced by the corresponding mutant strains are described and discussed in the context of the available structural models of FeMo-cofactor and its polypeptide environment.

It was also previously concluded, on the basis of information gained from a spectroscopic technique called electron spin echo envelope modulation, that the observed N-coordination of FeMo-cofactor requires the α-histidine-195 residue (Thomann *et al.*, 1991). Structural studies have revealed that the α-histidine-442 residue rather than the α-histidine-195 residue is covalently coordinated to FeMo-cofactor. In the accompanying paper, the effect of amino-acid substitutions on the electron spin echo envelope modulation elicited from protein-bound FeMo-cofactor has been revisited and extended.

EXPERIMENTAL PROCEDURES

Mutant Strain Construction. Methods for site-directed mutagenesis, gene replacement, and isolation of mutant strains were performed as described or cited previously (Brigle *et al.*, 1987; Jacobson *et al.*, 1989). The isolation of strain DJ528 was described previously (Scott *et al.*, 1990). A mixed set of oligonucleotides having the sequence 5′TCCCAGTCCCTGGGCXXXCACATCGCCAACGAC3′ was used for mutagenesis of the *nifD* gene during construction of other mutant strains. XXX indicates degenerate positions within the mixed oligonucleotide set and corresponds to the 195^{His} codon within the *nifD* gene sequence (Brigle *et al.*, 1985). For clarity in presentation, strains are indicated by both a numerical designation and the amino acid that occupies the MoFe protein α-subunit-195 position. For example, DJ527 (α-195^{His}) designates the parental strain used in the construction of mutants strains. It produces wild-type MoFe protein having a histidine residue at the α-subunit-195 position. This strain also contains a deletion and an insertion mutation within the *hoxKG* gene cluster (Menon *et al.*, 1990) such that uptake hydrogenase activity is eliminated. Mutants were constructed using a parental strain having *hoxKG* deleted so that nitrogenase-catalyzed hydrogen-evolution activities could be accurately measured in crude extracts without interference from uptake hydrogenase activity. The plasmid necessary for construction of DJ527, pALMZ′1, was kindly provided by Rob Robson.

Preparation of Crude Extracts and Nitrogenase Purification. Techniques for culturing *A. vinelandii*, media preparation, nitrogenase derepression, preparation of crude extracts, anaerobic purification of nitrogenase, and maintaining anoxic conditions were performed as previously described or cited by Scott *et al.* (1992). Isolation of nitrogenase component proteins from crude extracts prepared from DJ527 (α-195^{His}, the isogenic parental strain) and DJ540 (α-195^{Gln}) was performed as follows. Heat-treated crude extracts (heat treatment was either at 56 °C for 5 min for the wild-type crude extract or at 50 °C for 5 min for the mutant crude extract) were prepared in a degassed 25 mM Tris buffer, pH 7.4, made anoxic by the addition of 1 mM $Na_2S_2O_4$ and loaded on a 5 × 15 cm Pharmacia Q-sepharose column using a peristaltic pump. Flow rates for all column chromatography procedures were maintained at approximately 8 mL/min. After washing the loaded protein sample with two column volumes of the above buffer, the nitrogenase component proteins were eluted using a linear NaCl gradient (0.1−0.7 M) controlled by Pharmacia FPLC pumps. Under these conditions, both the wild-type and altered MoFe proteins eluted at approximately 0.37 M NaCl and Fe protein eluted at approximately 0.6 M NaCl. The partially purified MoFe protein was then brought to 0.5 M $(NH_4)_2SO_4$ by the addition of an appropriate amount of a degassed $(NH_4)_2SO_4$ stock solution (1.0 M in 25 mM Tris buffer, pH 7.4) made anaerobic by the addition of 1.0 mM $Na_2S_2O_4$ and loaded on a 3 × 15 cm Pharmacia phenyl-Sepharose column pre-equilibrated with degassed 25 mM Tris buffer (pH 7.4) containing 1 mM $Na_2S_2O_4$ and 0.5 M $(NH_4)_2SO_4$. A linear, decreasing $(NH_4)_2SO_4$ gradient (0.5−0 M) eluted the MoFe protein at about 0.1 M $(NH_4)_2SO_4$. The MoFe protein was then concentrated in an Amicon microfiltration cell concentrator fitted with an XM30 membrane using approximately 20 psi Ar pressure. The residual $(NH_4)_2SO_4$ was removed by repeated dilution and concentration of the sample using degassed 25 mM Tris, pH 7.4, 0.25 M NaCl, and 1 mM $Na_2S_2O_4$ buffer as the diluent. The Fe protein fraction obtained from the Q-Sepharose column was also concentrated

as described for the MoFe protein and was of sufficient purity at this stage for the described studies. Purity of protein samples was determined by gel electrophoresis using modifications of the procedure described by Laemmli (1970) as discussed by Scott *et al.* (1992).

Electron Paramagnetic Resonance Spectroscopy. Derepressed whole cells of wild-type and the various mutant strains were treated individually in 50 mM Tris, pH 8.0, with 5 mM $Na_2S_2O_4$ and 0.1 mM methyl viologen under argon for 5 min. The suspension was then transferred under anoxic conditions to a degassed, capped EPR tube. After centrifugation at 600*g* for 5 min, the supernatant was removed and the contents of the EPR tube frozen in liquid nitrogen. The EPR spectra of whole-cell preparations were recorded at 9.22 GHz and 5 mW on a Varian Associates E-line spectrometer with a 100-kHz field modulation of 10 G at 12 K maintained by liquid helium boil-off. The EPR spectra of purified wild-type and α-195^{Gln} MoFe proteins were recorded under identical spectral conditions, except the microwave power was 20 mW and the 100-kHz field modulation was 25 G.

Assays and Preparation of Gases for Kinetic Experiments. MoFe protein and Fe protein specific activities were respectively measured in crude extracts in the presence of an added optimal amount of the separately purified, complementary component protein. Acetylene- and proton-reduction activities were assayed in 9.25-mL reaction vials fitted with butyl rubber stoppers and aluminum seals. Each 1.0-mL reaction volume contained 25 mM TES, pH 7.4, 2.5 mM ATP, 5.0 mM $MgCl_2$, 30 mM creatine phosphate, 0.125 mg of creatine phosphokinase, and 20 mM $Na_2S_2O_4$. A gas mixture of either 10% C_2H_2/90% Ar or 100% Ar was used for determination of acetylene reduction and proton reduction, respectively. For crude extract assays, the reaction was started by the addition of 50 μL of crude extract and terminated after incubation at 30 °C for 8 min by injecting 0.25 mL of 2.5 M H_2SO_4. Ethylene and ethane production was quantified by gas chromatography using a Poropak N column and a FID detector (Shimadzu, Tokyo, Japan). H_2 evolution was also quantified by gas chromatography using a molecular sieve 5A column (Supelco, Bellefonte, PA) and a TCD detector. Calibrations were performed using standard gases of 1 ppm C_2H_4, 1 ppm C_2H_6, or 1% H_2 (Scott Specialty Gasses, Plumsteadville, PA). Activities of purified MoFe proteins were measured under conditions of high electron flux using 0.075 mg of MoFe protein and 0.925 mg of Fe protein per each reaction. These concentrations represent a mole ratio of approximately 40 Fe protein:1 MoFe protein. Assays were performed as described above except that the reactions were started by addition of purified MoFe protein. For the determination of kinetic parameters, gas mixtures of the desired concentrations were prepared individually in each assay vial using gas stocks in 60-mL serum vials. Gas-tight syringes (Hamilton, Reno, NV) with 22-gauge hypodermic needles were used to mix and transfer the gases. The very small amounts of CO required for some experiments involved prior serial dilution in Ar before mixing with the other gases. Total pressure in all assay vials was 1 atm. After the gas mixtures were prepared, assays were performed as described above. Nitrogen-reduction assays were performed in 35 mM HEPES buffer, pH 7.4, because the TES buffer used in the other assays interferes with the NH_3 analysis. In these assays, N_2 reduction was terminated by the addition of 0.25 mL of 0.4 M EDTA, pH 8.0. Each reaction mixture was then individually applied to a Bio-Rad Dowex 1-X2 ion-exchange column (Dilworth *et al.*, 1992) before being assayed for NH_3 by the indophenol method (Chaney & Marbach, 1962). Hydrolysis of MgATP during nitrogenase turnover was also measured from the liquid sample collected from the Dowex column by the creatine assay as previously described (Dilworth *et al.*, 1992; Ennor, 1957). Assays for hydroxylamine and hydrazine formation were performed as described by Novak and Wilson (1948) and Thorneley *et al.* (1978), respectively. In experiments designed to determine whether or not N_2 is a reversible inhibitor of proton reduction, each MoFe protein was first assayed for H_2-evolution activity under either an Ar or a N_2 atmosphere at 30 °C. After 5 min each reaction vial was then degassed and filled with Ar and reincubated at 30 °C for an addition 8 min. All reactions were terminated by the addition of 0.25 mL of 2.5 M H_2SO_4.

Table 1: Nif Phenotypes of α-195^{His} Mutant Strains and MoFe Protein and Fe Protein Activities in Crude Extracts from Those Strains

strain[a]	substitution at α-195	codon	Nif phenotype	MoFe specific activity[b] C_2H_4	MoFe specific activity[b] C_2H_6	MoFe specific activity[b] H_2	Fe specific activity[b] H_2
DJ527	WT (His)	CAC	+	45.3	0.0	64.0	35.8
DJ528	Asn	AAC	−	3.7	1.0	13.0	36.4
DJ538	Tyr	UAU	−	5.5	0.0	20.7	23.3
DJ540	Gln	CAA	−	30.7	0.0	48.8	36.0
DJ542	Leu	UUA	−	11.7	0.2	22.0	49.7
DJ544	Thr	ACA	−	2.8	0.0	18.2	27.1
DJ546	Gly	GGG	−	2.6	0.0	16.1	33.1

[a] All strains are deleted for the uptake hydrogenase structural genes. WT indicates the parental wild type strain. [b] Crude extract specific activity is expressed as nmol of C_2H_4, C_2H_6, or H_2 produced/min/mg of total extract protein. C_2H_4 and C_2H_6 were produced under a 10% C_2H_2/90% Ar atmosphere, and H_2 was produced under a 100% Ar atmosphere in the presence of saturating levels of purified complementary protein.

RESULTS

Diazotrophic Growth Characteristics and Nitrogenase Catalytic Activities in Crude Extracts. Site-directed mutagenesis and gene-replacement procedures were used to construct six different *A. vinelandii* mutant strains, each of which produces an altered MoFe protein having an individual amino-acid substitution located at the α-subunit-195 position occupied by a histidine residue in the wild-type strain. Each of these individual substitutions (Asn, Tyr, Gln, Leu, Thr, and Gly) results in a strictly Nif$^-$ phenotype in the corresponding mutant strain (Table 1). Crude extracts prepared from nitrogenase-derepressed wild-type and mutant strains were assayed for nitrogenase component−protein activities, and the results of these assays are compared in Table 1. All strains constructed in the present study were prepared in a *hoxKG* background (see Experimental Procedures) so that proton-reduction activities could be accurately measured in crude extracts. It should be noted that, because crude extracts are prepared from nitrogenase-derepressed cells, it is difficult to accurately compare activities of the MoFe protein in different preparations without an estimate of the relative levels of nitrogenase derepression. In the present experiments, estimation of the relative levels of nitrogenase accumulation in crude extracts from different strains was accomplished by either comparison of one-dimensional gel

Table 2: CO and N_2 Inhibition of H_2 Evolution Catalyzed by Crude Extracts Prepared from Wild-Type and α-195^{His} Mutant Strains

substitution at α-195	specific activity[a] of H_2 evolution under		
	100% Ar	10% CO/90% Ar	100% N_2
WT (His)	66.0	61.0	19.4
Asn	12.8	15.0	12.2
Gln	53.7	48.6	18.8
Leu	27.8	25.8	32.1
Thr	23.5	10.7	18.2

[a] Specific activity is expressed as nmol of H_2 produced/min/mg of crude extract protein assayed in the presence of optimal levels of purified Fe protein.

electrophoresis profiles (data not shown) or measuring the corresponding levels of Fe protein activity (Table 1). Because the relative levels of accumulation of the nitrogenase components were shown to be roughly equal by these measurements, quantitative differences in MoFe protein specific activities present in different mutant strain crude extracts can be attributed to specific alterations in their respective MoFe proteins. Although none of the mutant strains is able to fix N_2 at a level sufficient to support diazotrophic growth, crude extracts prepared from the mutant strains exhibited various levels of acetylene- and proton-reduction activities. These properties are particularly striking in the case of DJ540 (α-195^{Gln}) where acetylene- and proton-reduction activities were respectively 67% and 76% of the corresponding wild-type activities.

We have previously shown that MoFe protein from DJ528 (α-195^{Asn}) catalyzes the reduction of acetylene by both two and four electrons to yield ethylene and ethane (Scott *et al.*, 1992), an activity not exhibited by wild-type. Mutant strain crude extracts were, therefore, examined for their ability to produce both ethylene and ethane (Table 1). We found that extracts from DJ528 (α-195^{Asn}) and DJ542 (α-195^{Leu}) are able to reduce acetylene to both ethylene and ethane, but extracts from wild-type and the other mutant strains can only reduce acetylene by two electrons to yield ethylene. The possibility that ethane formation catalyzed by extracts from DJ528 and DJ542 results from the activity of a V-dependent nitrogenase was eliminated by spectroscopic, electrophoretic, and catalytic considerations as described previously (Dean *et al.*, 1990a; Scott *et al.*, 1990).

Effect of CO and N_2 on MoFe Protein-Catalyzed Proton Reduction. In previous studies, we have shown that certain amino-acid substitutions located within FeMo-cofactor-binding domains result in proton reduction that is sensitive to CO (Scott *et al.*, 1992). For example, substitution of the α-glutamine-191 residue by lysine results in MoFe protein-catalyzed proton-reduction activity that is about 50% inhibited by CO (Scott *et al.*, 1992), whereas, wild-type MoFe protein-catalyzed proton reduction is insensitive to CO (Hardy *et al.*, 1965; Bulen *et al.*, 1965). Results summarized in Table 2 show that the DJ544 MoFe protein (α-195^{Thr}) also exhibits CO-sensitive proton-reduction activity but proton reduction catalyzed by the altered MoFe protein from the other mutant strains examined is insensitive to CO.

The observation that various amino-acid substitutions placed at the α-195 position result in MoFe proteins, which exhibit detectable acetylene- and proton-reduction activities but are apparently unable to reduce N_2 (see later results), raises the question of whether or not these altered MoFe proteins have the ability to bind N_2. To investigate this possibility, we asked if N_2 is able to inhibit proton reduction catalyzed by the mutant strain crude extracts. These experiments revealed that N_2 causes marked, but reversible, inhibition of proton reduction catalyzed by either wild-type MoFe protein (α-195^{His}) or DJ540 MoFe protein (α-195^{Gln}). In contrast, N_2 does not significantly inhibit proton reduction catalyzed by altered MoFe protein from the other mutant strains (Table 2).

Whole-Cell EPR Spectra. The electron paramagnetic resonance (EPR) spectra of whole cells of the mutant strains all exhibit line shapes that are similar to wild-type (data not shown). However, the spectra of strains DJ542 (α-195^{Leu}), DJ528 (α-195^{Asn}), and DJ546 (α-195^{Gly}) exhibit greatly diminished EPR intensity (10%, 8%, and 3%, respectively, of wild-type). The apparent g values of these samples are also slightly shifted with respect to those of wild-type. In contrast, the whole-cell EPR spectrum of DJ540 (α-195^{Gln}) has an intensity comparable to wild-type but is more rhombic with apparent g values of 4.36 and 3.64. Compared with the other strains studied, these changes represent only a mild modification in the whole-cell EPR signal of DJ540 (α-195^{Gln}) indicating only a slight perturbation in the FeMo-cofactor environment caused by the substitution. The changed EPR signals from the various altered nitrogenases are correlated with changes in their corresponding catalytic properties, a correlation that supports the idea that FeMo-cofactor is located at or is part of the substrate-reduction site. However, although a rough correlation exists between EPR signal intensity and H_2-evolution activity, no obvious correlation exists between the EPR changes and either the ability to produce ethane from acetylene or the sensitivity of proton reduction to CO (see Tables 1 and 2).

Purification and EPR Analysis of α-195^{Gln} MoFe Protein from DJ540. Crude extract activity measurements show that the α-195^{Gln} MoFe protein is able to efficiently reduce both protons and acetylene. In contrast, although the α-195^{Gln} MoFe protein is apparently able to bind N_2, it is unable to reduce it to yield NH_3. Thus, the α-195^{Gln} MoFe protein was purified in order to further characterize its catalytic properties and determine whether or not it is able to reduce N_2 to a product other than NH_3. MoFe protein produced by both the wild-type (α-195^{His}) and DJ540 (α-195^{Gln}) was purified in parallel from crude extracts using a three-step procedure involving a heat step, anion-exchange chromatography, and hydrophobic interaction chromatography. One-dimensional SDS polyacrylamide gel electrophoretic analyses of the wild-type and α-195^{Gln} MoFe proteins purified in this way reveal only two bands, which correspond to the α- and β-subunits of the MoFe protein (Figure 2).

For unambiguous interpretation of the experiments described in the following sections, it was important to establish that any differences in the catalytic properties of the α-195^{Gln} MoFe protein, when compared to the wild-type MoFe protein, can be ascribed to genuine changes in catalytic properties rather than to changes arising from an artifact of the purification procedure. This concern was addressed in several ways. First, the line shape and the g values of the EPR spectra from the purified MoFe proteins were compared to their respective whole-cell EPR spectra. Neither the line shape nor the enhanced rhombic character around $g \approx 4$ of the EPR spectrum of α-195^{Gln} MoFe protein changed during purification, indicating that the altered MoFe protein was

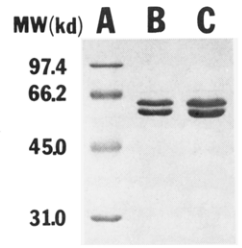

FIGURE 2: SDS−PAGE of purified wild-type and α-Gln-195 MoFe proteins. Lane A, molecular weight standard markers—phosphorylase b (97 400), bovine serum albumin (66 200), ovalbumin (45 000), and carbonic anhydrase (31 000); lane B, wild-type MoFe protein; lane C, α-195^{Gln} MoFe protein.

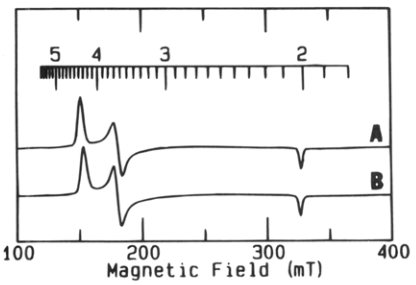

FIGURE 3: EPR spectra of purified α-195^{Gln} MoFe protein (A) and purified wild-type MoFe protein (B). Each sample contains approximately 40 mg/mL purified MoFe protein.

not compromised structurally, compositionally, or functionally during the purification process. Second, a quantitative comparison of the EPR spectra of the purified wild-type and α-195^{Gln} MoFe proteins shows that, although the respective EPR line shape and *g* values are slightly changed when the two proteins are compared, their intensities are about the same (Figure 3). Thus, although the FeMo-cofactor polypeptide environment of the α-195^{Gln} MoFe protein is somewhat different than that of the wild-type MoFe protein, a feature also revealed by whole-cell EPR spectra, the α-195^{Gln} MoFe protein apparently has a full complement of FeMo-cofactor. Third, several of the catalytic properties of the α-195^{Gln} MoFe protein were monitored during different stages of purification. For example, the relative levels of acetylene-reduction and proton-reduction activities, the insensitivity of proton reduction to CO, and the sensitivity of proton reduction to N_2 did not change during purification.

The α-195^{Gln} MoFe Protein Does Not Reduce N_2. Like the wild-type MoFe protein, α-195^{Gln} MoFe protein exhibits N_2 inhibition of proton reduction. In the wild-type, such inhibition of proton reduction caused by N_2 can be explained by diversion of electrons to N_2 reduction resulting in NH_3 formation. However, DJ540, which produces the altered α-195^{Gln} MoFe protein, is incapable of diazotrophic growth so it is impossible that N_2 inhibition of proton reduction catalyzed by the altered MoFe protein is a consequence of NH_3 formation. This conclusion was independently confirmed by our inability to detect NH_3 production from N_2 catalyzed by the purified α-195^{Gln} MoFe protein. The possibility that the α-195^{Gln} MoFe protein is able to catalyze reduction of N_2 to yield some other nitrogenous product was also examined. Because there is evidence that hydrazine is formed as a bound intermediate during the course of N_2 reduction catalyzed by nitrogenase, we tested for its formation by using the acid-quenched reaction assay previously described by Thorneley *et al.* (1978). Hydroxylamine was also sought as a potential product, although it is neither a natural product of wild-type nitrogenase catalysis nor an intermediate formed during NH_3 formation. Hydrazine was detected during nitrogenase turnover from acid-quenched samples of wild-type MoFe protein at a level comparable to that previously reported (Thorneley *et al.*, 1978; Dilworth & Eady, 1991), but the α-195^{Gln} MoFe protein was found incapable of catalyzing the production of any detectable hydrazine formation. As expected, neither the wild-type nor the α-195^{Gln} MoFe protein were able to catalyze formation of hydroxylamine.

To determine whether or not N_2 is a reversible inhibitor of both acetylene reduction and proton reduction catalyzed by the α-195^{Gln} MoFe protein, the following experiment was devised. Proton-reduction activity was first assayed under an N_2 atmosphere. Then, the reaction vessel was flushed with Ar and proton reduction assayed a second time but now under an Ar atmosphere. Near full recovery of proton reduction was achieved after replacing N_2 with Ar, demonstrating that N_2 binding to the altered MoFe protein is reversible. The reversible nature of N_2 binding to both the wild-type and α-195^{Gln} MoFe proteins also became evident in the kinetic analyses described below.

N_2 Inhibition of Electron Flux to Proton Reduction in the α-195^{Gln} MoFe Protein Uncouples MgATP Hydrolysis from Substrate Reduction. Although neither hydrazine nor hydroxylamine was produced by the α-195^{Gln} MoFe protein, the possibility that it reduces N_2 to some other unknown product remained a plausible explanation for N_2 inhibition of proton reduction. This possibility was eliminated by the results of proton-reduction assays performed under either an Ar or a N_2 atmosphere and under conditions of limiting reductant, in this case $Na_2S_2O_4$ (Figure 4). The rationale for this experiment is that, upon exhausting the source of reductant, it should be possible to trace all the available electrons to specific product formation. Panel A of Figure 4 shows that, under N_2, the wild-type MoFe protein distributes approximately 75% of the available electron flux to NH_3 production and 25% of electron flux to proton reduction. This conclusion is apparent by comparing the total amount of H_2 produced under an Ar atmosphere versus H_2 produced under an N_2 atmosphere. The distribution of electron flux to H_2 formation and NH_3 formation, when wild-type MoFe protein was assayed under N_2, was separately confirmed in an experiment where all the products were quantified. In addition, the allocation of electrons to specific products, when wild-type MoFe protein is assayed under an N_2 atmosphere, has been well established by other investigators [see, for example, Burris (1991), Lowe and Thorneley (1984)]. In contrast, panel B of Figure 4 shows that, in the case of the α-195^{Gln} MoFe protein, N_2 does not divert electron flux to form products other than H_2 but instead slows the overall rate of proton reduction. Namely, all of the available reducing equivalents are ultimately accounted for by H_2 formation whether catalysis occurs under either an Ar or a N_2 atmosphere.

In a different series of experiments, proton reduction catalyzed by the wild-type and α-195^{Gln} MoFe proteins was measured under conditions of limiting MgATP under either an Ar or a N_2 atmosphere (Figure 5). As discussed above for the condition of limiting reductant, a decrease in the amount of H_2 produced by wild-type MoFe protein catalysis under a N_2 atmosphere compared to an Ar atmosphere can also be accounted for by diversion of electron flux to NH_3

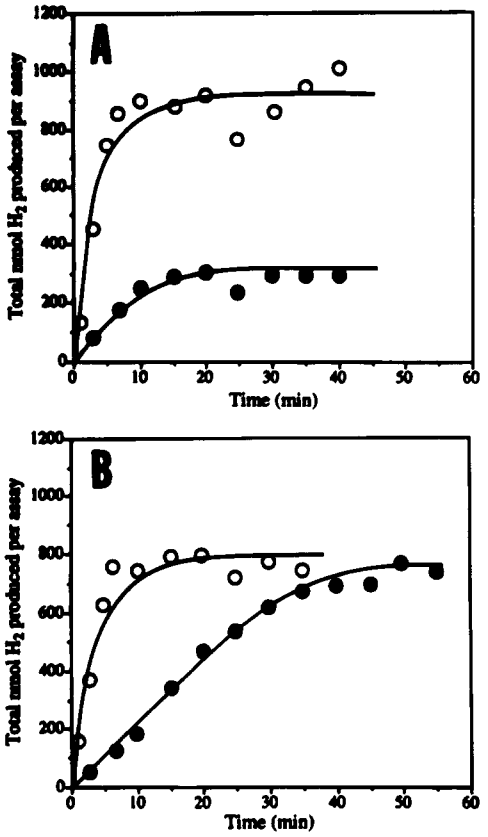

FIGURE 4: Time course of H_2 evolution catalyzed by purified wild-type MoFe protein (A) and purified α-195^{Gln} MoFe protein (B) under limiting concentrations of $Na_2S_2O_4$ under either 100% Ar (open circles) or 100% N_2 (closed circles) atmosphere. The assay conditions were as described in Experimental Procedures except that the initial $Na_2S_2O_4$ concentration was 1 μmol/1 mL of total reaction mixture.

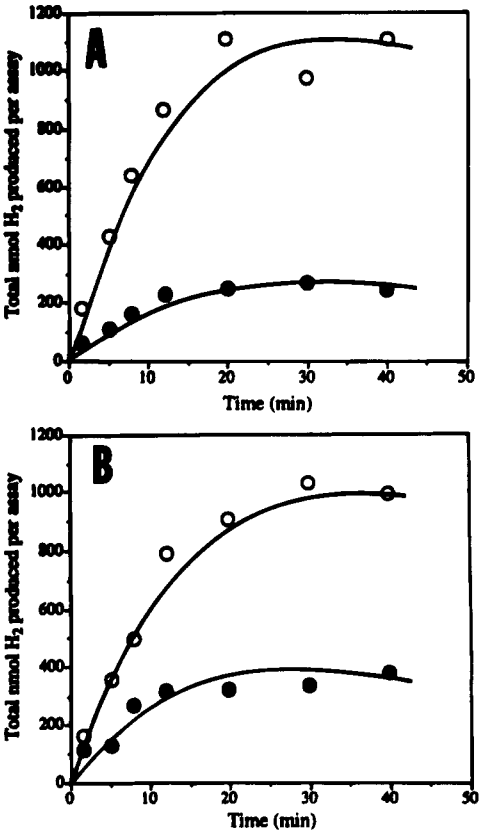

FIGURE 5: Time course of H_2 evolution catalyzed by purified wild-type MoFe protein (A) or purified α-195^{Gln} MoFe protein (B) under limiting concentrations of MgATP under either 100% Ar (open circles) or 100% N_2 (closed circles) atmosphere. The assay conditions were as described in Experimental Procedures except that the initial MgATP concentration was 5 μmol/1 mL of total reaction mixture with no ATP-regenerating system present.

formation. Again, this assumption was separately confirmed in other experiments where NH_3 production was also monitored. In contrast to the condition of limiting reductant, where the α-195^{Gln} MoFe protein ultimately catalyzes the same amount of H_2 production under either an Ar or a N_2 atmosphere, MgATP limitation resulted in a lowered level of H_2 production when catalysis occurred under a N_2 atmosphere than when under an Ar atmosphere (Figure 5, panel B). Thus, in the case of the α-195^{Gln} MoFe protein, N_2 uncouples MgATP hydrolysis from electron transfer. This feature of the α-195^{Gln} MoFe protein was found to be true whether or not MgATP was limiting. These results are summarized in Table 3 where it is shown that wild-type MoFe protein hydrolyzes about 5.0 MgATP for each electron pair delivered to substrate reduction (i.e., about 5 MgATP/2e$^-$) when assayed under either an Ar or a N_2 atmosphere. In contrast, the α-195^{Gln} MoFe protein hydrolyzes approximately 5.4 MgATP/2e$^-$ when assayed under Ar but hydrolyzes about 23 MgATP/2e$^-$ when assayed under N_2.

Determination of Kinetic Parameters. N_2 is not a substrate for the α-195^{Gln} MoFe protein, yet it is an inhibitor of both proton and acetylene reduction. This feature allowed determination of the binding affinity of both N_2 and acetylene for the substrate-reduction site and also allowed determination of the pattern of N_2 inhibition of acetylene reduction by the altered MoFe protein. These parameters were determined by measuring acetylene-reduction rates as a function of acetylene concentration in the presence of various fixed concentrations of N_2. A series of Lineweaver–Burk plots generated from these measurements is shown in Figure 6. These results show that N_2 is a "competitive" inhibitor of acetylene reduction catalyzed by either the wild-type or the α-195^{Gln} MoFe protein, exhibiting K_i values of 0.219 and 0.357 atm, respectively [see Davis and Wang (1980) for a detailed discussion on the nature of N_2 inhibition of acetylene reduction]. The K_m values for acetylene binding are 0.005 atm for the wild-type MoFe protein and 0.006 atm for the α-195^{Gln} MoFe protein. In these experiments, H_2 produced during catalysis did not interfere with N_2 inhibition of acetylene reduction because the acetylene concentrations (>1%) were sufficiently high to suppress H_2 evolution to minimal levels. The possibility that H_2 produced by catalysis might interfere with N_2 inhibition of acetylene reduction was considered because H_2 is known to inhibit N_2 reduction (Wilson & Umbreit, 1937).

Table 3: Kinetic Parameters[a] and ATP/2e$^-$ Ratio of Wild-Type and α-195^{Gln} MoFe Protein

MoFe protein	K_m C_2H_2[b]	K_i N_2[b]	K_i CO[c]	ATP/2e$^-$ under 100% Ar	ATP/2e$^-$ under 100% N_2
wild-type	0.005	0.219	0.00033	4.8	5.5
α-Gln-195	0.006	0.357	0.00004	5.4	23.0

[a] K_m and K_i values were obtained from the Lineweaver–Burk plots using a computer program (EZ-FIT) and are expressed in atmospheres. [b] K_m C_2H_2 and K_i N_2 values were obtained from Figure 6. [c] K_i CO values represent average values obtained from Figures 7 and 8.

Because the patterns of CO inhibition of both acetylene reduction and N_2 binding might be altered by the α-195^{Gln}

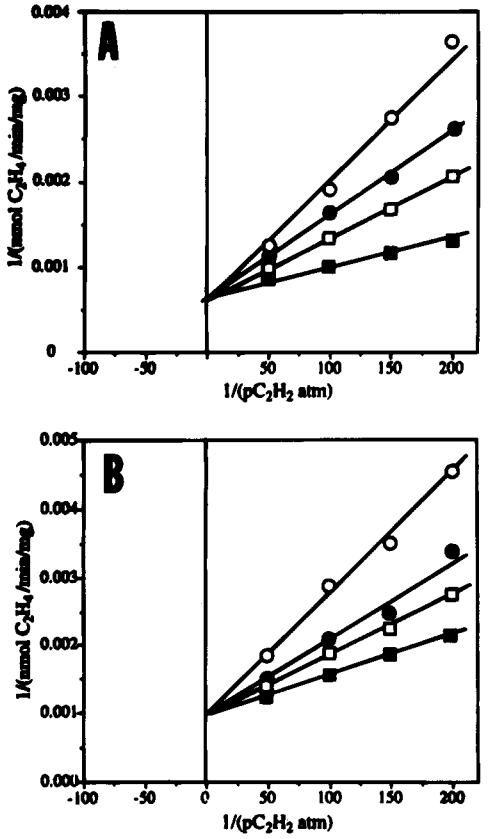

FIGURE 6: N_2 inhibition of acetylene reduction catalyzed by purified wild-type MoFe protein (A) or purified α-195^{Gln} MoFe protein (B). The graph represents a series of Lineweaver–Burk plots where the reciprocal of the acetylene-reduction specific activity is plotted against the reciprocal of the acetylene concentration. Each plot was determined in the presence of a fixed level of N_2: p_{N_2} = 0 atm (filled squares), 0.2 atm (open squares), 0.4 atm (filled circles), and 0.6 atm (open circles).

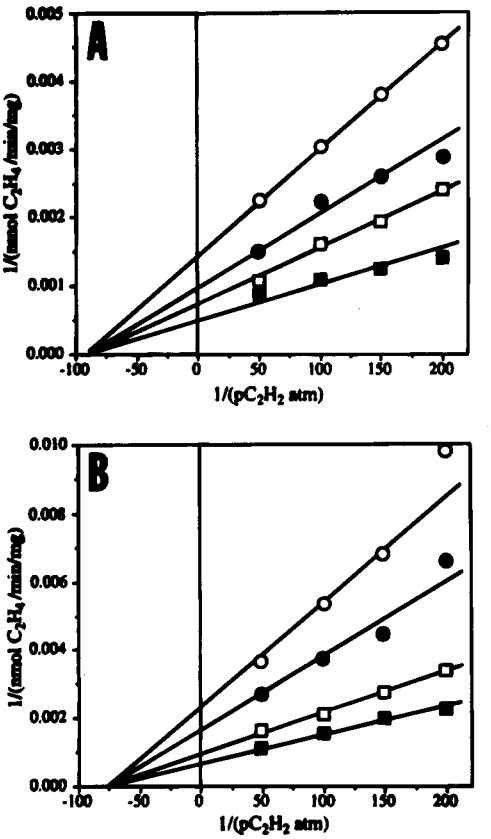

FIGURE 7: CO inhibition of acetylene reduction catalyzed by purified wild-type MoFe protein (A) or purified α-195^{Gln} MoFe protein (B). The graph represents a series of Lineweaver–Burk plots where the reciprocal of the C_2H_2-reduction specific activity is plotted against the reciprocal of the C_2H_2 concentration. For panel A, each plot was determined in the presence of the following fixed level of CO: p_{CO} = 0 atm (filled squares), 0.00015 atm (open squares), 0.00025 atm (filled circles), and 0.0005 atm (open circles). For panel B, each plot was determined in the presence of the following fixed level of CO: p_{CO} = 0 atm (filled squares), 0.000025 atm (open squares), 0.000063 atm (filled circles), and 0.0001 atm (open circles).

substitution, the appropriate comparisons with wild-type MoFe protein were run. Acetylene-reduction rates were measured as a function of substrate concentration with various fixed concentrations of CO (Figure 7). In Figure 8, CO inhibition of N_2 binding was determined by monitoring proton reduction when assayed in the presence of both N_2 and CO. These latter experiments provide an indirect way to examine CO binding to the altered MoFe protein by asking whether or not CO is able to reverse the inhibition by N_2 of proton reduction. The results show that, for both the wild-type and α-195^{Gln} MoFe protein, CO is a noncompetitive inhibitor of both acetylene reduction and N_2 binding. These data also permitted calculation of the corresponding K_i values for CO and an estimation of the K_m values for acetylene binding independent from that obtained from data presented in Figure 6. CO was found to be a much more potent inhibitor of acetylene reduction catalyzed by the α-195^{Gln} MoFe protein (K_i = 0.00004 atm) when compared to the wild-type MoFe protein (K_i = 0.00033 atm). K_m values for acetylene binding calculated from these data (0.008 atm for the wild-type MoFe protein and 0.012 atm for the α-195^{Gln} MoFe protein; see Figure 7) are somewhat higher than calculated from the data shown in Figure 6. It should be noted that the K_m values determined from N_2 inhibition of acetylene reduction (Figure 6) are probably more accurate than those determined from the CO-inhibition experiments (Figure 7) because the low level of CO used in the latter experiments required serial dilution of the stock gas, thus introducing the possibility of errors in the estimation of CO in the reaction vessel. Nevertheless, all of the values fall within the range of those published previously (Dilworth, 1966; Hardy *et al.*, 1971; Hwang & Burris, 1972; Hwang *et al.*, 1973; Rivera-Ortiz & Burris, 1975; Schollhorn & Burris, 1967).

DISCUSSION

Our results provide insight concerning the nature of the interaction of the substrates, N_2, acetylene, and protons, and the inhibitor CO with the nitrogenase substrate-reduction site. It has been known for many years that N_2 is a potent inhibitor of both proton and acetylene reduction catalyzed by wild-type nitrogenase (Rivera-Ortiz & Burris, 1975). However, because N_2 is also a substrate for nitrogenase, it was not known heretofore whether or not N_2 inhibits reduction of other substrates by binding at a separate site and then competing for the available reducing equivalents or by competing for occupancy of the same active site. The observation that N_2 is not reduced by the α-195^{Gln} MoFe protein but effectively inhibits both proton reduction and acetylene reduction suggests that N_2 is able to compete with both acetylene and protons for active site occupancy. Although these results do not rule out the formal possibility

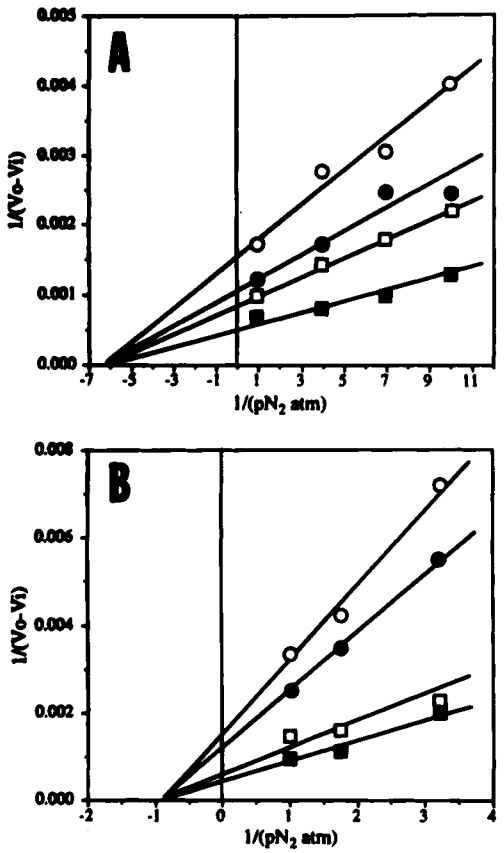

FIGURE 8: CO inhibition of N_2 binding to purified wild-type MoFe protein (A) or purified α-195^{Gln} MoFe protein (B). The specific activity for H_2 evolution (nmol H_2 produced/min/mg of MoFe protein) decreases upon binding of N_2, and this suppression is inhibited by CO. Therefore, CO inhibition of N_2 binding was determined in the absence of N_2 reduction by measuring H_2 evolution. H_2 evolution was measured with increasing p_{N_2} at fixed levels of p_{CO}. When the difference between H_2-evolution specific activities under no p_{N_2} and a given p_{N_2} ($V_o - V_i$) was plotted against p_{N_2} at fixed levels of p_{CO}, a series of curves similar in shape to the Michaelis–Menten curves were obtained. H_2 evolution of 2000 nmol produced/min/mg of MoFe protein, which was measured under no p_{N_2} and no p_{CO}, was used as V_o. Resulting double-reciprocal plots are shown above. For panel A, each plot was determined in the presence of the following fixed level of CO: p_{CO} = 0 atm (filled squares), 0.00015 atm (open squares), 0.00025 atm (open circles), and 0.0005 atm (filled circles). For panel B, each plot was determined in the presence of the following fixed level of CO: p_{CO} = 0 atm (filled squares), 0.000025 atm (open squares), 0.000063 atm (filled circles), and 0.0001 atm (open circles).

that different substrates bind to the active site in different ways, bind at different subsites within the active site, or bind at different redox states, the results do show that the different substrates tested cannot bind and be reduced at the active site at the same time. In addition, the K_m values for acetylene and the K_i values for N_2 are only marginally different when the wild-type and α-195^{Gln} MoFe proteins are compared. These similarities indicate that the ability of N_2 to inhibit both proton and acetylene reduction exhibited by the α-195^{Gln} MoFe protein is probably mechanistically relevant.

Another interesting feature of the α-195^{Gln} MoFe protein is that it exhibits a marked increase in susceptibility to CO inhibition of acetylene reduction and N_2 binding compared to the wild-type (see Figures 7 and 8 and Table 3). Two different possibilities for the decreased K_m for CO of the altered MoFe protein can be considered. The first possibility comes from a structural consideration where substitution of the α-histidine-195 residue by a glutamine residue simply makes a potential CO-binding site more accessible. Inspection of the polypeptide environment surrounding FeMo-cofactor shows that the α-histidine-195 residue is positioned such that the ε-nitrogen of its imidazole group is able to participate in forming an NH→S hydrogen bond with a bridging sulfide. In this arrangement, the imidazole ring is positioned so that a neighboring Fe within FeMo-cofactor (see Figure 1), designated Fe2 in the molecular models of both Kim and Rees (1992a) and Bolin *et al.* (1993), would normally be sterically protected. Consequently, the steric protection of this Fe might either make it inaccessible to attack by CO or force CO to bind in an unfavorable geometry. Thus, although substitution of the α-histidine-195 position by glutamine would still permit formation of an NH→S hydrogen bond to the bridging sulfide, it could result in loss of this steric protection for Fe2 of FeMo-cofactor. This latter possibility has biochemical precedence in the case of CO reactivity with the heme Fe of hemoglobin (Collman *et al.*, 1976). However, on the basis of the available molecular model of the MoFe protein structure, it does not appear obvious that substitution of glutamine for the α-histidine-195 residue would either make any Fe atom contained within FeMo-cofactor more accessible to attack by CO or result in a polypeptide environment that favors a geometry more suitable for stabilization of the metal–CO bond. Clearly, a satisfactory structural explanation for the increased sensitivity of the α-195^{Gln} MoFe protein to CO will require determination of the three-dimensional structure of the altered protein. Nevertheless, the present results, which show that certain substitutions can result in proton reduction that is partially sensitive to CO (Table 2) whereas a different substitution results in an altered MoFe protein having proton reduction insensitive to CO but exhibiting increased CO inhibition of acetylene reduction or N_2 binding (Figures 7 and 8), suggest that there is more than one CO-binding site located on or near the FeMo-cofactor. Indeed, the available published data suggest that there are at least two different CO-binding sites located within the MoFe protein (Davis *et al.*, 1979), yet neither of these sites has been pinpointed. In this regard, it is also noted that the absence of any appreciable effect of the α-195^{Gln} substitution on the K_m values for both acetylene binding and N_2 binding suggests that their binding site is somewhat remote from that for CO, which is in line with the usual interpretation of the noncompetitive pattern of CO inhibition.

An electronic argument might also be considered in an attempt to explain the higher level of CO sensitivity of the α-195^{Gln} MoFe protein. Replacement of the NH→S hydrogen bond to the bridging sulfide provided by the α-histidine-195 residue by a corresponding NH→S hydrogen bond from the substituting glutamine residue is expected to shift the redox potential of FeMo-cofactor in a slightly negative direction. However, it is unlikely that a small shift in redox potential could have such a dramatic effect on the susceptibility of one or more of the metal sites to attack by CO. On the other hand, any change in the electronic properties of FeMo-cofactor caused by the glutamine substitution could have a profound effect on the ability of the α-195^{Gln} MoFe protein to reduce N_2 by rendering the MoFe protein incapable of sufficiently lowering the unfavorable activation energy of the initial electron transfer to N_2. In this context, it is noted that there is a considerable network of NH→S

hydrogen bonds to the FeMo-cofactor sulfides, and they have already been suggested as possible contributors toward stabilization of intermediates formed during substrate reduction (Kim & Rees, 1992b; Bolin *et al.*, 1993). Because the α-195^{Gln} MoFe protein is able to effectively reduce protons and acetylene, both of which require only two electrons, we favor a model where the NH→S hydrogen bond provided by the α-histidine-195 residue functions to stabilize an early, partially reduced intermediate, most likely a hydrazido^{2-} or diazene species, that is likely formed during the course of the six-electron reduction of N_2.

During nitrogenase turnover, the Fe protein cycles between the 2^+ and 1^+ redox states through which it sequentially delivers single electrons to the MoFe protein in a process that requires association and dissociation of the two component proteins and hydrolysis of probably two MgATP per electron transfer. Because multiple electrons are required for substrate reduction, the association and dissociation of the Fe protein and the various reduced forms of the MoFe protein must be coordinated so that electron flow occurs mainly in one direction. Several different features might contribute to this aspect of nitrogenase catalysis. First, a switching mechanism has been proposed to operate where, following MgATP hydrolysis and intermolecular electron transfer, the MgADP-bound Fe protein assumes a conformation that helps prevent electron back-flow to the Fe protein (Wolle *et al.*, 1992). Second, the presence of two different redox-active centers within the MoFe protein might serve to achieve an intramolecular distribution of the accumulated electrons. Third, the substrate itself could assist in ensuring the quasi-unidirectional flow of electrons by acting as a molecular sink.

Our results with the α-195^{Gln} MoFe protein provide evidence that electron capture by the substrate during turnover does indeed play a critical role in controlling the direction of electron flow during nitrogenase catalysis. This conclusion is supported by the following properties of the α-195^{Gln} MoFe protein: (i) N_2 is able to effectively bind at the active site; (ii) N_2 is not reduced; (iii) N_2 slows the rate of proton reduction; and (iv) N_2 uncouples MgATP hydrolysis from electron transfer without substantialy altering the overall rate of MgATP hydrolysis. A simple explanation for these results is that because N_2 occupies the substrate-reduction site, but cannot be reduced, electrons accumulated within the α-195^{Gln} MoFe are ultimately back-donated to an oxidized form of the Fe protein [see discussion by Orme-Johnson *et al.* (1977)]. A related possibility is that, once the altered MoFe protein becomes saturated with electrons that cannot be sequestered by substrate reduction, the two components retain their ability to associate and effect MgATP hydrolysis but are unable to achieve intermolecular electron transfer. This possibility is supported by evidence that MgATP hydrolysis precedes intermolecular electron transfer (Thorneley *et al.*, 1989), although MgATP-dependent proton release appears to be slower than electron transfer (Mensink *et al.*, 1992). It is important to emphasize that N_2 does not appreciably slow the rate of MgATP hydrolysis in these experiments, so it is unlikely that binding of N_2 to the α-195^{Gln} MoFe protein has any effect on component−protein interaction.

The uncoupling of MgATP hydrolysis and electron transfer is a familiar feature of nitrogenase enzymology. For example, conditions of high or low pH, high or low temperature (Imam & Eady, 1980; Jeng *et al.*, 1970; Watt *et al.*, 1975), low electron flux resulting from high MoFe protein-to-Fe protein ratios (Eady & Postgate, 1974; Hageman & Burris, 1978), and certain amino-acid substitutions that alter component−protein interaction (Lowery *et al.*, 1989; Wolle *et al.*, 1992) have all been shown to uncouple MgATP hydrolysis and electron transfer. These phenomena have also been explained as manifestations of futile cycling of electrons. The key difference in the present study is that a small molecule, N_2, uncouples a system that otherwise exhibits relatively efficient coupling of MgATP hydrolysis and proton reduction. A similar situation is found in the cases of CH_3NC and HCN/CN^-, which have also been shown to uncouple MgATP hydrolysis from electron flow to the wild-type MoFe protein (Li *et al.*, 1982; Rubinson *et al.*, 1983). Uncoupling of MgATP and electron flow caused by these compounds is somewhat more complicated, however, because they are both nitrogenase substrates (CH_3NC and HCN) and inhibitors (CH_3NC and CN^-). Most importantly, the uncoupling caused by CH_3NC and HCN/CN^- does not have a dramatic effect on the overall rate of MgATP hydrolysis. Thus, it appears that uncoupling of MgATP hydrolysis and electron flow caused by all of these small molecules is likely to be a consequence of blocking electron transfer to the ultimate electron sink, the substrate.

A *structural* role for the α-histidine-195 residue became evident from experiments where the N_2 susceptibilities of proton reduction catalyzed by the various mutant strains were compared. In these experiments, N_2 inhibition of proton-reduction activity is an obvious indication that the altered MoFe protein retains the ability to bind N_2. Conversely, the inability of N_2 to inhibit proton reduction catalyzed by certain mutant strains is interpreted to indicate that the substrate-binding site has been modified such that effective N_2 binding is not possible. Thus, the data summarized in Table 2 show that the α-195^{Gln} MoFe protein is distinguished from the other altered MoFe proteins in retaining the ability to bind N_2. The significant structural difference observed when glutamine is compared to the other substituting amino acids is that only the glutamine substitution retains the potential to form a NH→S hydrogen bond through its amide N to the appropriate bridging sulfide of FeMo-cofactor in a configuration similar to that normally provided by the imidazole ϵ-nitrogen of the α-histidine-195 residue. This feature is illustrated in Figure 1, where the ϵ-nitrogen of the α-histidine-195 residue is approximately 3.14 Å from the bridging sulfide. It is, therefore, likely that a NH→S hydrogen bond to the bridging sulfide provided by either a histidine or a glutamine residue can function in positioning the FeMo-cofactor within the polypeptide pocket, such that the substrate-binding site retains affinity for N_2, whereas the other substituting amino acids are unable to fulfill this role. It is also probable that small changes in the EPR line shape and *g* values, as well as the ability to either reduce acetylene to ethane or exhibit CO-sensitive proton reduction as observed for certain of the altered MoFe proteins, are manifestations of a reorientation of FeMo-cofactor within the polypeptide pocket. Another important finding is that, while whole cells of both the wild-type and α-195^{Gln} strain exhibit similar EPR intensities and, therefore, probably have similar complements of FeMo-cofactor, whole-cell EPR intensities of the other mutant strains are generally much lower. Such results indicate that MoFe proteins from these other mutant strains probably do

not have a full complement of FeMo-cofactor. Thus, it appears that the NH→S hydrogen bond provided by the α-histidine-195 residue is likely to function not only in correctly positioning FeMo-cofactor for substrate binding and reduction but also in assisting in binding FeMo-cofactor within the polypeptide.

In summary, we come to the following conclusions. First, an altered MoFe protein, which is able to bind but cannot reduce N_2, has been characterized. N_2 is able to inhibit acetylene reduction and proton reduction catalyzed by this altered MoFe protein without competing for the available reducing equivalents, which suggests that N_2 inhibits both acetylene and proton reduction by simple occupation of a common substrate-binding site. Second, although the binding of N_2 to the altered MoFe protein uncouples MgATP hydrolysis from proton reduction, it does not affect the overall rate of MgATP hydrolysis. This result provides evidence that the substrate ordinarily plays a significant role in controlling the direction of electron flow during nitrogenase turnover by serving as an effective electron sink and, thereby, avoiding the futile cycling of electrons. Third, replacement of the α-histidine-195 residue by glutamine results in a dramatic increase in the apparent affinity for CO by the altered protein. Although the most reasonable interpretation of this result is that the imidazole group of the α-histidine-195 residue might normally protect the Fe_2 atom of FeMo-cofactor from attack by CO, molecular modeling of the α-195^{Gln} MoFe protein does not provide compelling support for this hypothesis. Finally, comparison of the altered substrate binding and spectroscopic and catalytic properties of MoFe proteins from the various mutant strains provides evidence that a NH→S hydrogen bond involving the imidazole ϵ-nitrogen of the α-histidine-195 residue has a structural role in correctly positioning FeMo-cofactor within the polypeptide matrix and a catalytic role in fine tuning the electronic properties of the substrate binding and reduction site. Further electrochemical and structural analyses of the α-195^{Gln} MoFe protein, now in progress, should provide additional details concerning the role of the important α-histidine-195 residue in nitrogenase catalysis.

ACKNOWLEDGMENT

We thank Claudia Vigil for help in mutant strain constructions, Dick Dunham for performing EPR spectroscopy, and Jeff Bolin and Steve Muchmore for helpful discussions and computer modeling.

REFERENCES

Bolin, J. T., Campobasso, N., Muchmore, S. W., Morgan, V. T., & Mortenson, L. E. (1993) in *Molybdenum Enzymes, Cofactors and Model Systems* (Stiefel, E. I., Coucouvanis, D., & Newton, W. E., Eds.) pp 186−195, American Chemical Society, Washington, DC.

Brigle, K. E., Newton, W. E., & Dean, D. R. (1985) *Gene 37*, 37−44.

Brigle, K. E., Setterquist, R. A., Dean, D. R., Cantwell, J. S., Weiss, M. C., & Newton, W. E. (1987) *Proc. Natl. Acad. Sci. U.S.A. 84*, 7066−7069.

Bulen, W. A., Burns, R. C., LeComte, J. R., & Hinkson, J. (1965) in *Non-Heme Iron Proteins: Role in Energy Conversion* (San Pietro, A., Ed.) pp 261−274, Antioch Press, Yellow Springs, OH.

Burris, R. H. (1991) *J. Biol. Chem. 266*, 9339−9342.

Chan, M. K., Kim, J., & Rees, D. C. (1993) *Science 260*, 792−794.

Chaney, A. L., & Marbach, E. P. (1962) *Clin. Chem. 8*, 130−132.

Collman, J. P., Brauman, J. I., Halbert, T. R., & Suslick, K. S. (1976) *Proc. Natl. Acad. Sci. U.S.A. 73*, 3333−3337.

Davis, L. C., & Wang, Y.-L. (1980) *J. Bacteriol. 141*, 1230−1238.

Davis, L. C., Henzl, M. T., Burris, R. H., & Orme-Johnson, W. H. (1979) *Biochemistry 18*, 4860−4869.

Dean, D. R., & Jacobson, M. R. (1992) in *Biological Nitrogen Fixation* (Stacey, G., Burris, R. H., & Evans, H. J., Eds.) pp 763−834, Chapman & Hall, New York and London.

Dean, D. R., Scott, D. J., & Newton, W. E. (1990a) in *Nitrogen Fixation: Achievements and Objectives* (Gresshoff, P. M., Roth, L. E., Stacey, G., & Newton, W. E., Eds.) pp 95−102, Chapman & Hall, New York and London.

Dean, D. R., Setterquist, R. A., Brigle, K. E., Scott, D. J., Laird, N. F., & Newton, W. E. (1990b) *Mol. Microbiol. 4*, 1505−1502.

Dean, D. R., Bolin, J. T., & Zheng, L. (1993) *J. Bacteriol. 175*, 6737.

Dilworth, M. J. (1966) *Biochim. Biophys. Acta 127*, 285−294.

Dilworth, M. J., Eady, R. R. (1991) *Biochem. J. 277*, 465−468.

Dilworth, M. J., & Eldridge, M. E., & Eady, R. R. (1992) *Anal. Biochem. 207*, 6−10.

Eady, R. R., & Postgate, J. R. (1974) *Nature 249*, 804−910.

Ennor, A. H. (1957) *Methods Enzymol. 3*, 850−856.

Georgiadis, M. M., Komiya, H., Chakrabarti, P., Woo, D., Kornuc, J. J., & Rees, D. C. (1992) *Science 257*, 1653−1659.

Hageman, R. V., & Burris, R. H. (1978) *Biochemistry 17*, 4117−4124.

Hardy, R. W. F., Knight, E., Jr., & D'Eustachio, A. J. (1965) *Biochem. Biophys. Res. Commun. 20*, 539−544.

Hardy, R. W. F., Burns, R. C., & Parshall, G. W. (1971) in *Bioorganic Chemistry* (Gould, R. F., Ed.) pp 219−247, American Chemical Society, Washington D. C.

Hawkes, T. R., McLean, P. A., & Smith, B. E. (1984) *Biochem. J. 217*, 317−321.

Hoover, T. R., Imperial, J., Ludden, P. W., & Shah, V. K. (1989) *Biochemistry 28*, 2768−2771.

Hwang, J. C., & Burris, R. H. (1972) *Biochim. Biophys. Acta 283*, 339−350.

Hwang, J. C., Chen, C. H., & Burris, R. H. (1973) *Biochim. Biophys. Acta 292*, 256−270.

Imam, S., & Eady, R. R. (1980) *FEBS Lett. 110*, 35−38.

Jacobson, M. R., Cash, V. L., Weiss, M. C., Laird, N. F., Newton, W. E., & Dean, D. R. (1989) *Mol. Gen. Genet. 219*, 49−57.

Jeng, D. Y., Morris, J. A., & Mortenson, L. E. (1970) *J. Biol. Chem. 245*, 2809−2813.

Kim, J., & Rees, D. C. (1992a) *Science 257*, 1682.

Kim, J., & Rees, D. C. (1992b) *Nature 360*, 553−560.

Kim, J., & Rees, D. C. (1994) *Biochemistry 33*, 389−397.

Kim, J., Woo, D., & Rees, D. C. (1993) *Biochemistry 32*, 7104−7115.

Kraulis, P. (1991) *J. Appl. Crystallogr. 24*, 946−950.

Laemmli, U. K. (1970) *Nature 227*, 680−685.

Li, J.-G., Burgess, B. K., & Corbin, J. L. (1982) *Biochemistry 21*, 4393−4402.

Lowe, D. J., & Thorneley, R. N. F. (1984) *Biochem. J. 224*, 877−886.

Lowery, R. G., Chang, C. L., Davis, L. C., McKenna, M.-C., Stephens, P. J., & Ludden, P. W. (1989) *Biochemistry 28*, 1206−1212.

McLean, P. A., Smith, B. E., Dixon, R. A. (1983) *Biochem. J. 211*, 589−597.

Menon, A. L., Stults, L. W., Robson, R. L., & Mortenson, L. E. (1990) *Gene 96*, 67−74.

Mensink, R. E., Wassink, H., & Haaker, H. (1992) *Eur. J. Biochem. 208*, 289−294.

Novak, R., & Wilson, P. W. (1948) *J. Bacteriol. 55*, 517−524.

Orme-Johnson, W. H., Davis, L. C., Henzl, M. T., Averill, B. A., Orme-Johnson, N. R., Munck, E., & Zimmerman, R. (1977) in *Recent Developments In Nitrogen Fixation* (Newton, W. E., Postgate, J. R., & Rodriguez-Barrueco, C., Eds.) pp 131−178, Academic Press, London, New York, and San Francisco.

Rawlings, J., Shah, V. K., Chisnell, J. R., Brill, W. J., Zimmermann, R., Munck, E., & Orme-Johnson, W. H. (1978) *J. Biol. Chem. 253*, 1001−1004.

Rivera-Ortiz, J. M., & Burris, R. H. (1975) *J. Bacteriol. 123*, 537−545.

Rubinson, J. F., Corbin, J. L., & Burgess, B. K. (1983) *Biochemistry 22*, 6260−6268.

Schollhorn, R., & Burris, R. H. (1967) *Proc. Natl. Acad. Sci. U.S.A. 58*, 213−216.

Scott, D. J., May, H. D., Newton, W. E., Brigle, K. E., & Dean, D. R. (1990) *Nature 343*, 188−190.

Scott, D. J., Dean, D. R., & Newton, W. E. (1992) *J. Biol. Chem. 267*, 20002−20010.

Shah, V. K., & Brill, W. J. (1977) *Proc. Natl. Acad. Sci. U.S.A. 74*, 3249−3253.

Thomann, H., Bernardo, M., Newton, W. E., & Dean, D. R. (1992) *Proc. Natl. Acad. Sci. U.S.A. 88*, 6620−6623.

Thorneley, R. N. F., Eady, R. R., & Lowe, D. J. (1978) *Nature 272*, 557−558.

Thorneley, R. N. F., Ashby, G. A., Howarth, J. V., Millar, N. C., & Gutfreund, H. (1989) *Biochem. J. 264*, 657−661.

Watt, D. G., Bulen, W A., Burns, A., & Hadfield, K. L. (1975) *Biochemistry 14*, 4266−4272.

Wilson, P. W., & Umbreit, W. W. (1937) *Arch. Mikrobiol. 8*, 440−457.

Wolle, D., Kim, C., Dean, D. R., & Howard, J. B. (1992) *J. Biol. Chem. 267*, 3667−3673.

BI941396S